

See discussions, stats, and author profiles for this publication at: <https://www.researchgate.net/publication/3156693>

# Evaluation of the Propagation Model Recommendation ITU-R P.1546 for Mobile Services in Rural Australia

Article in IEEE Transactions on Vehicular Technology · February 2008

DOI: 10.1109/TVT.2007.901902 · Source: IEEE Xplore

---

CITATIONS

47

READS

4,331

3 authors, including:



Hajime Suzuki

The Commonwealth Scientific and Industrial Research Organisation

101 PUBLICATIONS 1,088 CITATIONS

[SEE PROFILE](#)



Hans-Jürgen Zepernick

Blekinge Institute of Technology

417 PUBLICATIONS 4,031 CITATIONS

[SEE PROFILE](#)

# Evaluation of the Propagation Model Recommendation ITU-R P.1546 for Mobile Services in Rural Australia

Erik Östlin, *Student Member, IEEE*, Hajime Suzuki, *Member, IEEE*, and Hans-Jürgen Zepernick, *Member, IEEE*

**Abstract**—In this paper, the validity of Recommendation ITU-R P.1546 in a short-range terrestrial environment is analyzed. Its three versions (P.1546, P.1546-1, and P.1546-2) are compared against simple models and evaluated using measurement results that were obtained by utilizing the pilot signal of a commercial code-division multiple-access mobile telephone network. Measurement results show that P.1546-2, on average, underestimates the field strength by more than 10 dB for typical Australian rural areas. However, it improves the error standard deviation compared to previous versions. The causes of these effects and the suggestions for further development of the Recommendation are discussed and evaluated.

**Index Terms**—Field strength measurements, Okumura–Hata model, point-to-area, propagation prediction, Recommendation ITU-R P.1546.

## I. INTRODUCTION

THE USE of mobile phone systems has seen a tremendous increase in the last decade. This increase is expected to continue in the areas of wireless broadband services, in which each user requires a larger bandwidth to support higher data rates with better quality of service. A careful planning of cell structure is therefore required to maximize the use of available spectrum in such systems. To enable realistic cell planning, path loss models and prediction tools that incorporate the characteristics of the particular region in which a system is intended to be deployed are required.

To address the growing need for industry-accepted propagation models for predicting reliable service areas and co-channel interference in the 800/900 MHz frequency range, the IEEE Vehicular Technology Society Committee on Radio Propagation was established to study radio propagation models and to make appropriate recommendations. Well-known propagation models, such as the Bullington [1], [2], Longley–Rice [3], and

Manuscript received April 28, 2006; revised February 13, 2007 and March 19, 2007. This paper was presented in part at the 63rd IEEE Vehicular Technology Conference, Melbourne, Australia, May 2006. This work was supported by the Commonwealth of Australia under the Cooperative Research Centre Program. The review of this paper was coordinated by Prof. D. Michelson.

E. Östlin is with Sensear Pty. Ltd., Perth, WA 6009, Australia (e-mail: erik.ostlin@sensear.com).

H. Suzuki is with the Commonwealth Scientific Industrial Research Organisation Information and Communication Technologies Centre, Marsfield, NSW 2122, Australia (e-mail: hajime.suzuki@csiro.au).

H.-J. Zepernick is with the Blekinge Institute of Technology, 372 25 Ronneby, Sweden (e-mail: hans-jurgen.zepernick@bth.se).

Digital Object Identifier 10.1109/TVT.2007.901902

Okumura [4] models, were evaluated against each other, against simple models, and against measurement data. The conclusion of the study at the time was that none of the evaluated models were accurate enough to warrant a recommendation [5]. This has prompted further effort to seek a standard method that is universally applicable and reliable.

For the purpose of improving the accuracy in predicting propagation path loss over irregular terrain, various methods, which are often computationally intensive, have been proposed in the literature. These methods include the use of the geometrical theory of diffraction [6], integral equation [7], and parabolic equation [8]. In the past, these models were often excluded from the list of suitable candidates as the standard model due to their complex algorithms and computational requirements. However, with the ever-increasing computational power, these models are being increasingly used for radio network planning. Hence, an internationally agreed standard model that is built upon these models may be realized in the near future.

The Radiocommunication Sector of the International Telecommunication Union (ITU-R) has developed a new Recommendation on the method of point-to-area predictions for terrestrial services in the frequency range of 30–3000 MHz. It supersedes well-known Recommendations such as P.370 [9] and P.529 [10] (the modified Okumura–Hata method), which are used mainly for broadcasting and mobile services, respectively. Since Recommendation ITU-R P.1546, which is evaluated in this paper, introduces several novel concepts, such as the application of terrain clearance angle (TCA) within the distance of 10 km, verification of the model by actual measurement results is of great importance. The Recommendation serves as a standard in areas of spectrum management and radio technology and is constantly under development. The work has been undertaken by the ITU-R Working Party 3K, followed by an extensive international approval process. Note that Recommendation ITU-R P.1546 is considered to be a path general model that uses less information that is unique to each path compared to path specific models. Currently, the ITU-R Working Party 3K is developing a new recommendation that takes into account path specific information to greater extent.

The prediction of field strength in a terrestrial environment is a complex task, e.g., when obstruction by terrain and/or scattering from objects is involved. ITU-R's Recommendation P.1546 achieves this by considering the following: 1) the effective height of the transmitting/base antenna; 2) correction as a function of receiving/mobile antenna height; and 3) correction

as a function of TCA, among other factors. Various modeling methods have been proposed for each correction factor, which have been incorporated in different versions of the Recommendation [11]–[13].

In this paper, the three factors of Recommendation ITU-R P.1546, as previously introduced, are reviewed. The applicability of the correction for receiving/mobile antenna height (RAH) in a flat open rural area is analyzed by using the two-ray model [14]. The behavior of the TCA correction is highlighted by applying two versions of the Recommendation to flat terrain. The three versions of Recommendation ITU-R P.1546 are compared with measurement results that were obtained by utilizing the pilot signal of a commercial code division multiple access (CDMA [15]) mobile network in rural Australia, revealing their advantages and disadvantages. In addition, modifications to P.1546 are proposed and evaluated using some of the conventional empirical models, such as the free space model [14] and the Okumura–Hata (OH) model [16], as path loss prediction benchmarks. Note that, while P.1546 covers a wide range of different propagation scenarios, as explained in Section II, this paper focuses on its application to mobile services in rural areas.

This paper is organized as follows: In Section II, the P.1546 model and its three main components (effective transmitting/base antenna height, correction for receiving/mobile antenna height, and TCA correction) are reviewed. The evaluation results using a flat terrain model and the evaluation results using measurement data are presented in Sections III and IV, respectively. Modifications to the P.1546 model are proposed, discussed, and evaluated in Section V. Finally, the conclusions and a discussion for future work are presented in Section VI.

## II. RECOMMENDATION ITU-R P.1546

Previous ITU-R Recommendations, such as P.370 [9], P.529 [10], and P.1146 [17], provided different results for similar or even identical propagation scenarios. Hence, the P.1546 model was developed to overcome known limitations and to combine various methods into a single method. The ITU-R P.1546 model provides a set of curves and tables of field strength as a function of frequency (100 MHz, 600 MHz, and 2 GHz), distance, (1–1000 km), transmitting/base antenna height, (10–1200 m), time variability (50%, 10%, and 1%), location variability (1–99%), and path type (land, cold sea, warm sea, and mixed paths), at the height of the receiving/mobile antenna being equal to the representative height of ground cover. Fig. 1 shows one set of curves that is applicable for land paths and a nominal frequency that is equal to 600 MHz. A rigorous interpolation/extrapolation procedure is given to allow consistent prediction for any input values within the specified range. After this procedure, the prediction of field strength should be corrected for different receiving/mobile antenna heights, and the prediction accuracy may be enhanced by the application of TCA correction. In the evaluation that is presented in the sequel, the P.1546 models are implemented using a digital elevation map (DEM) with a 9 second resolution grid, which corresponds to approximately 250 m, which is

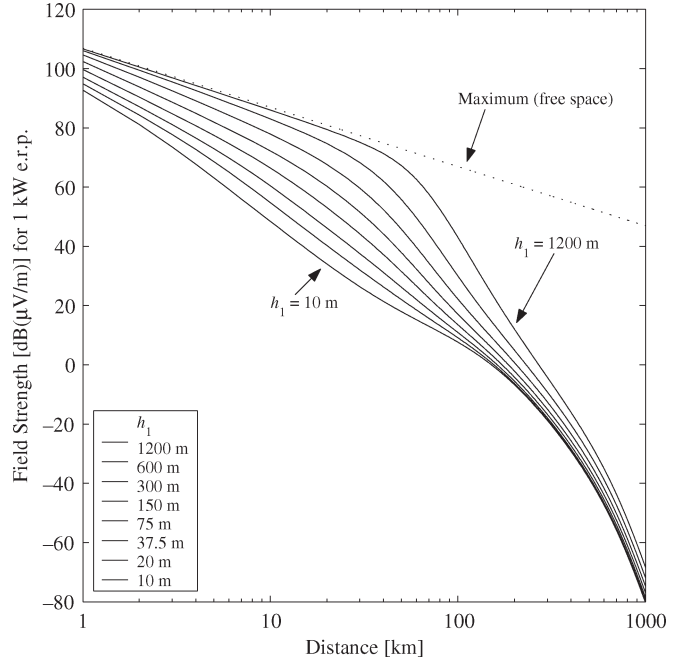


Fig. 1. P.1546 propagation curves for different transmitting/base antenna heights  $h_1$ , a nominal frequency of 600 MHz, land paths, 50% of time and locations, and receiving/mobile antenna height  $h_2$  at the representative clutter height  $R$ .

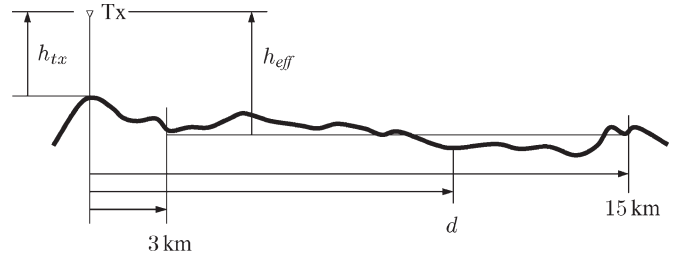


Fig. 2. Definition of effective antenna height  $h_{\text{eff}}$ .

supplied by Geoscience Australia. Note that the prediction accuracy produced by the models described in this paper may be improved by the use of a DEM with a finer resolution. However, such information is not readily available for the rural areas under investigation. The ITU-R P.1546 versions that are compared in this paper are the original P.1546 model, which is hereafter called P.1546-0 [11], P.1546-1 [12], and the latest version P.1546-2 [13].

### A. Transmitting/Base Antenna Height $h_1$

The  $h_1$  definition that is used in the P.1546 models is based on the definition of effective antenna height, as in the Okumura model [4]. Effective antenna height  $h_{\text{eff}}$  is calculated as the base station (BS) height in meters over the average level of the ground between distances  $d$  of 3 and 15 km in the direction of the mobile antenna (see Fig. 2).

1) *P.1546-0 Definition of  $h_1$ :* When  $d$  is larger than or equal to 15 km,  $h_1$  to be used in the model is simply  $h_{\text{eff}}$ . For path lengths that are less than 15 km,  $h_b$  is defined as the height in meters of the transmitting antenna above the terrain

height averaged between  $0.2d$  and  $d$  km. The transmitting/base antenna height is then calculated as

$$h_1 = h_a + \frac{(h_b - h_a)d}{15} \quad (1)$$

where  $h_a$  is the notional height of the transmitting/base antenna height above the clutter in its vicinity, and antenna heights  $h_1$ ,  $h_a$ , and  $h_b$ , and distance  $d$  are given in meters and kilometers, respectively. If the height above clutter is not available,  $h_a$  is defined as the antenna height above ground, i.e., the height of the mast  $h_{tx}$  (in meters). The method interpolates linearly (up to 15 km) between  $h_a$  and  $h_b$ , i.e., the method takes the physical height of the transmitting antenna into greater account when the receiving antenna is closer to the BS. This approach is, in practice, more robust against negative  $h_1$  values than the simplified method that is used in P.1546-1, as will be shown in Section IV.

2) *P.1546-1 Definition of  $h_1$ :* When the distance between the transmitting and receiving antennas is larger than or equal to 15 km, the base antenna height  $h_1$  to be used in the calculation is  $h_{eff}$ . For path lengths that are less than 15 km,  $h_1$  is equal to  $h_b$ . It is noted that this change in the transmitting/base antenna height definition was an effort to try to simplify the Recommendation.

3) *P.1546-2 Correction for Negative  $h_1$ :* The  $h_1$  definition in P.1546-2 is the same as that in P.1546-1, but for negative  $h_1$  values, a correction method that takes both diffraction and tropospheric scattering into account is introduced [13, Sec. 4.3]. It is noted that the method can result in a discontinuity in the predicted field strength at the transition around  $h_1 = 0$  m.

### B. Correction for Receiving/Mobile Antenna Height

The P.1546 prediction curves give field strength values for a reference receiving antenna at height  $R$  representing the height in meters of the ground cover surrounding the receiver. Examples of reference heights are given as follows:

- 30 m for dense urban areas;
- 20 m for urban areas;
- 10 m for suburban and rural areas.

The minimum reference height is 10 m. If the receiving antenna height  $h_2$  is different from  $R$ , a correction depending on the ground cover should be added. The correction curves that are presented in Fig. 3 are representative for  $f = 881.52$  MHz,  $d = 10$  km, and  $h_1 = 35$  m, which correspond to the pilot carrier frequency for a commercial CDMA system (IS-95) in Australia, the distance to BS, and the transmitting/base antenna height, respectively.

It can be seen in Fig. 3 that, for receiving antenna heights of approximately 1.44 m, the correction curves that correspond to rural and suburban areas intersect ( $-18.66$  dB), and for  $h_2 = 1$  m, the correction is larger for rural than for suburban areas. This leads to the conclusion that further investigations would be required to find a more appropriate correction for open rural areas. To investigate this matter further, the receiving antenna height correction that is used in Recommen-

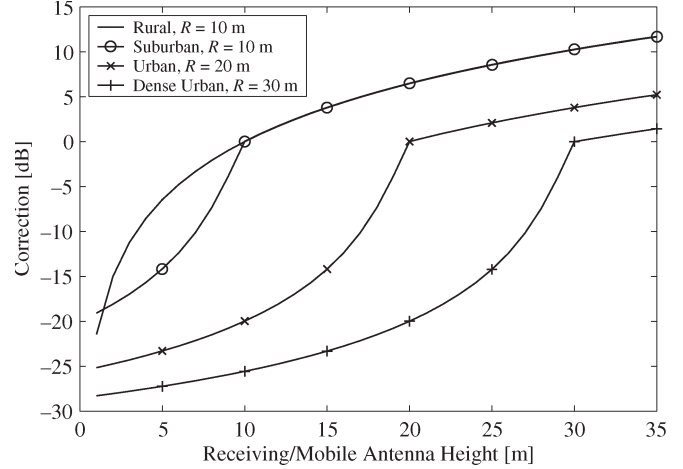


Fig. 3. Receiving/mobile antenna height correction curves for different land categories.

tion ITU-R P.370-7 and the two-ray model is introduced in Sections II-B1 and 2, respectively.

1) *P.370-7:* This ITU-R Recommendation uses gain correction  $c$  (in decibels) for different receiving antenna heights (1.5–40 m) relative to 10 m, which is calculated as

$$c = \frac{k}{6} \cdot 20 \log_{10} \left( \frac{h_2}{10} \right) \quad (2)$$

where parameter  $k$  is 4 dB for the ultrahigh frequency (UHF) band and rural areas. For example,  $c$  is about  $-10$  dB for  $h_2 = 1.7$  m, which is approximately 6.5 dB less than the P.1546-2 correction for the RAH for the same scenario.

2) *Two-Ray Model:* While it is acknowledged that Recommendation P.1546 is to be developed on the basis of empirical results, an analysis using the two-ray model [14] for flat ground was performed to develop a better understanding of the RAH correction. For the frequency under consideration (881.52 MHz) and for distances that are larger than 5 km, the correction curve for RAH agrees reasonably well with the two-ray model [see Fig. 4(a)]. It is noted that the P.1546 correction for the RAH is always greater than the correction that was obtained with the two-ray model for open flat ground. This may account for added propagation loss due to vegetation and clutter that typically surround the receiving/mobile antenna. For the described scenario and shorter distances (e.g.,  $< 2$  km), the received field strength according to the two-ray model does not necessarily decrease when lowering the receiving antenna [see Fig. 4(b)]. This may call for the development of distance-dependent RAH correction.

### C. Terrain Clearance Angle Correction

For land paths, TCA correction may be added to increase the prediction accuracy, enabling obstacles that are close to the receiver site to be taken into account. The correction is based on the TCA in degrees, which is given by

$$\theta_{tca} = \theta - \theta_r \quad (3)$$

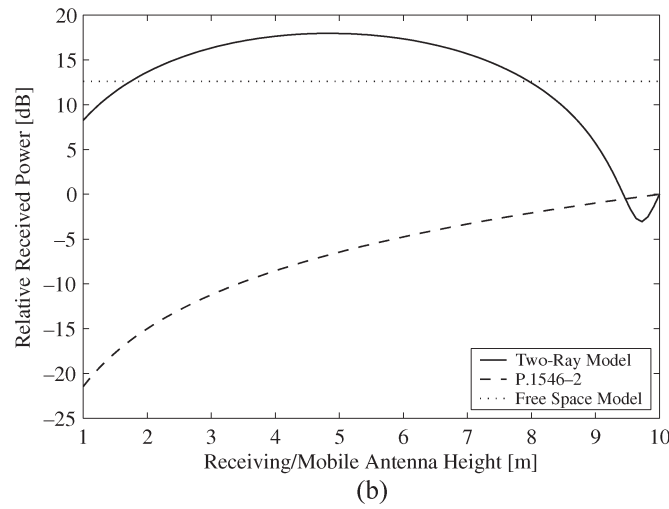
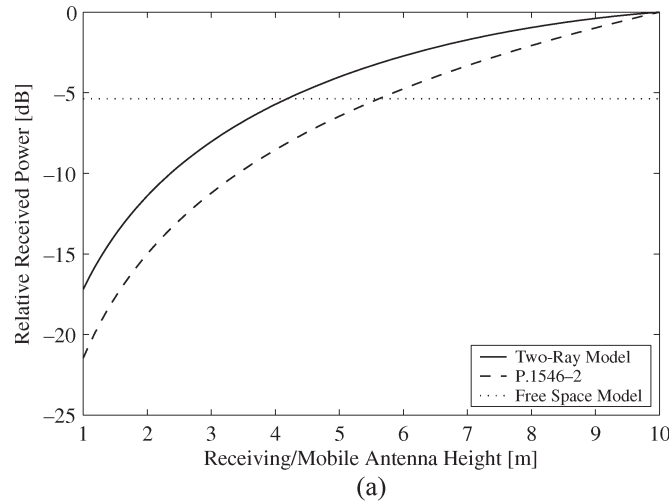


Fig. 4. Relative received power versus receiving/mobile antenna height for vertically polarized isotropic antennas, flat ground,  $h_1 = 35$  m, relative permittivity  $\epsilon_r = 15$ , and conductivity  $\sigma = 0.005$ . (a)  $d = 5$  km. (b)  $d = 2$  km.

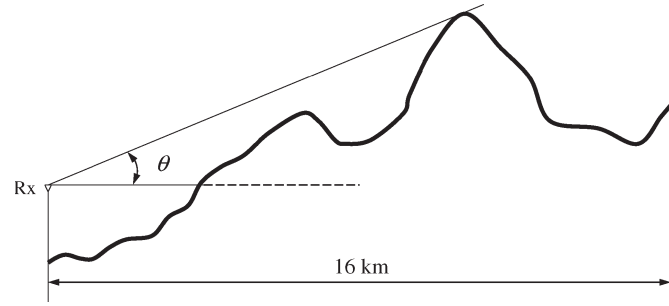


Fig. 5. Definition of  $\theta$  ( $d \geq 16$  km).

where  $\theta$  is measured relative to the horizontal at the mobile antenna, which clears all the terrain obstructions over a distance of up to 16 km but does not go beyond the base antenna (see Fig. 5).

Reference angle  $\theta_r$  is given by

$$\theta_r = \arctan \left( \frac{h_{1s} - h_{2s}}{1000 d} \right) \quad (4)$$

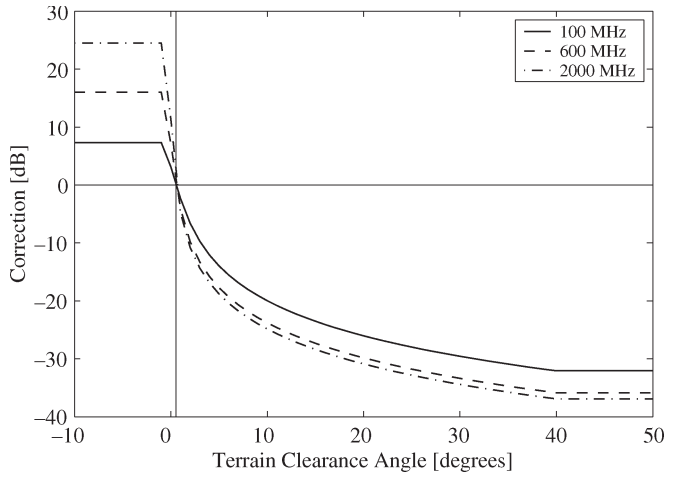


Fig. 6. TCA correction curves for nominal frequencies.

where  $h_{1s}$  and  $h_{2s}$  represent the heights of the base and mobile antennas in meters above sea level, respectively, and distance  $d$  is given in kilometers.

In P.1546-0 and P.1546-1, the higher and lower values of the TCA correction are limited by the values that are given at angles  $\theta_{tca} = -0.8^\circ$  and  $\theta_{tca} = 40^\circ$ . In P.1546-2, the lower  $\theta_{tca}$  limit was changed from  $-0.8^\circ$  to  $0.55^\circ$ , and the resulting effect is that no TCA correction is added for  $\theta_{tca} < 0.55^\circ$  (see Fig. 6). The P.1546-2 field strength predictions for flat rural scenarios therefore become more pessimistic compared to the predictions that were made by P.1546-0 and P.1546-1. In Fig. 6, the curves corresponding to 100 and 600 MHz are supported by P.370-7. The source of the 2000 MHz TCA correction curve is not known to the authors. In addition, in P.370-7, the TCA correction for UHFs never exceeds +18 dB, as it does in P.1546-1, and the curves were applicable only for distances ranging from 10 to 1000 km. Further development should therefore be aimed at making the TCA correction distance dependent for distances of less than 10 km. Furthermore, when the RAH is changed from its reference height, both the TCA and the RAH corrections are affected. While the TCA correction is measured from the receiving/mobile antenna height, the authors are of the opinion that the TCA should be measured from the reference height when the receiving/mobile antenna is surrounded by clutter since the line-of-sight (LOS) from the receiving/mobile antenna to the obstructing terrain is blocked by the clutter. How the TCA should be measured in open rural areas requires further discussion on taking into account how the TCA correction and the RAH correction interact with each other.

### III. EVALUATION BY MODEL

To investigate the behavior of the P.1546 models, comparisons with the well-known OH model were performed for flat rural areas. For comparison, the following field strength prediction curves are presented:

- P.1546 excluding corrections for TCA and RAH;
- P.1546 including TCA correction;
- P.1546 including RAH correction;
- P.1546 including TCA and RAH corrections (full model);
- OH models (rural, suburban, and urban).

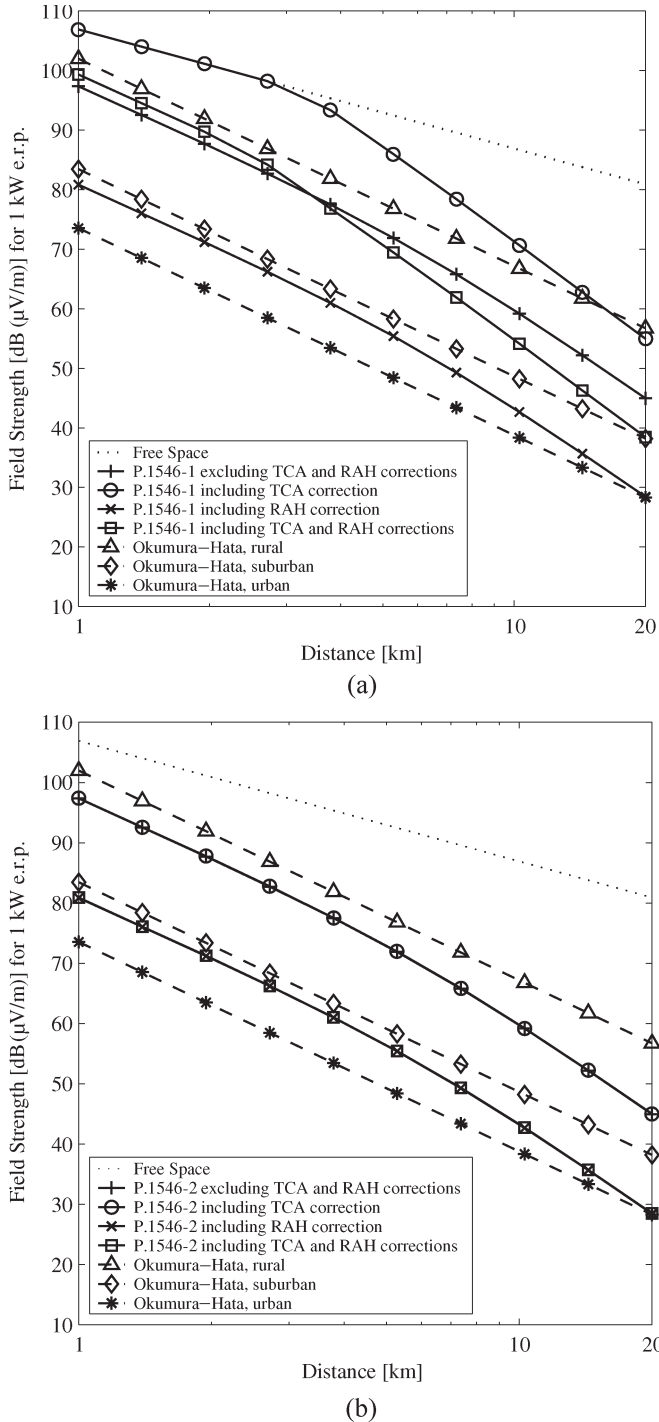


Fig. 7. Field strength prediction for flat rural areas. The model parameters for this scenario are  $f = 881.52$  MHz,  $h_1 = 35$  m, and  $h_2 = 1.7$  m. (a) P.1546-1. (b) P.1546-2.

It is noted that Recommendation ITU-R P.1546 is compatible with the OH model for certain urban scenarios [11]–[13]. It is also recognized that the OH method is based on measurements that are performed in urban areas, and to cater to suburban and rural areas, the model introduces correction factors (see [16]). In Fig. 7, the OH models are used as a benchmark that points out the different behaviors of the TCA corrections in P.1546-1 and P.1546-2, respectively. The field strength prediction results

for flat rural terrain using the P.1546-1 and P.1546-2 models can be seen in Fig. 7(a) and (b), respectively.

First, the TCA correction curves, as in P.1546-1, yield a positive correction when there are negative TCA angles (LOS scenario) and, therefore, correct the P.1546 field strength prediction curve by about 16 dB upward (circles), depending on TCA. For the P.1546-2 model, the TCA correction for the same flat rural scenario is 0 dB due to the changed lower TCA limit, as described in Section II-C. Second, the correction for the RAH corrects the P.1546 prediction at the height of representative clutter (plus signs) by about 16.5 dB downward (x marks), independent of the antenna separation distance. Note that the prediction results for P.1546-0 and P.1546-1 are almost identical for the described scenario.

In Fig. 7(a), it can be seen that the field strength predictions provided by the P.1546-1 full model (squares) are 2.5–15 dB lower than those provided by the OH rural model (triangles) for distances ranging from 1 to 20 km. It is well known that the OH model, in general, produces overly optimistic prediction results for open rural areas (see, e.g., [18, Sec. 4.3.3]); hence, the aforementioned behavior seems reasonable. Note that, for a flat scenario as previously given, the TCA depends on the distance between the transmitting and receiving antennas. As shown in Fig. 7(a), in the range of 1–3 km, the P.1546-1 predictions are limited in order to not exceed the predictions by the free space model.

In Fig. 7(b), it can be seen that the predictions provided by the P.1546-2 full model (squares) are 2.5–10 dB lower than those provided by the OH suburban model (diamonds) for distances ranging from 1 to 20 km. At 20 km, the prediction approaches the OH urban model, which does not seem to be intuitively correct. In P.1546-2, the TCA-dependent correction is 0 dB for negative TCA angles (typical LOS scenario) and, therefore, does not correct the P.1546 prediction curve (plus signs) at all. Therefore, the uncorrected P.1546 prediction curve (plus signs) is the same as the P.1546 prediction curve that was corrected for TCA (circles). The correction for the RAH reduces the P.1546 prediction at the height of representative clutter (plus signs) by about 16.5 dB (x marks). Hence, the P.1546-2 full model (squares) is identical to the curve that incorporates only the correction for the RAH (x marks). The full P.1546-2 model, including both TCA and RAH corrections, therefore predicts much lower field strengths for rural LOS scenarios compared to P.1546-1 and provides prediction results that are identical to P.1546-1 without TCA correction applied.

#### IV. EVALUATION BY MEASUREMENTS

In this section, the evaluation of the P.1546 versions using measurement data that were obtained by utilizing the IS-95 pilot signal in a commercial CDMA network in rural Australia is presented.

##### A. Measurement Procedure

Mobile radio wave propagation measurements were performed using a CDMA pilot scanner that was built by the Commonwealth Scientific and Industrial Research Organisation

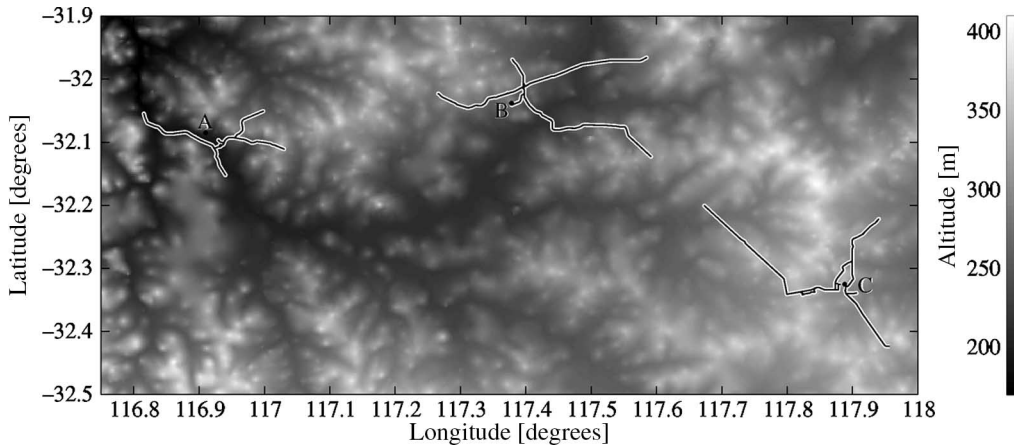


Fig. 8. Digital elevation map, using 9 second resolution, used for the point-to-area propagation model Recommendation ITU-R P.1546. The measurement data originates from 19 routes and three BSs with omnidirectional antenna characteristics in rural Western Australia. From left to right: The BSs Beverley, Quairading, and Corrigin are marked with a dot and A, B, and C, respectively.

(CSIRO) and the Australian Telecommunications Cooperative Research Centre (ATcrc). The scanner is controlled by a laptop personal computer and includes a global positioning system (GPS) receiver and an omni-directional antenna. During the measurements, the receiving antenna was placed on the roof of a car at a height of approximately 1.7 m above ground. The scanner is capable of tracking eight pilot signals simultaneously, and the correlation peak (the magnitude of the dominant path) of one pilot signal can be sampled at rates that are selectable down to 1/600 seconds, allowing tracking of fast signal fades.

The measurements originating from two measurement campaigns that were performed in rural Western Australia in June 2003 [19] and May 2004 [20] were analyzed and used for evaluating the P.1546 versions. The collected drive test data originate from three omni-directional BSs with macrocell characteristics [Beverley (A), Quairading (B), and Corrigin (C)] and cover more than 400 km of different rural terrains with different signal distributions. Nineteen measurement tracks from the area of interest that is plotted on a DEM, together with BS positions and altitude shown in meters, can be seen in Fig. 8. For large parts of the measurements, the LOS between the transmitting and receiving antennas was present, which resulted in negative TCAs. The data are therefore very suitable for evaluating and comparing the two different sets of TCA correction curves that were incorporated in P.1546-1 and P.1546-2, respectively. Typically, only one pilot channel was received at the same time in these rural areas, limiting the effect of inter-cell interference. The BS positions were given by the register of radiocommunications licenses held at the Australian Communications and Media Authority (ACMA). The transmitting pilot power, antenna height, and antenna pattern (omni-directional) of the BSs were provided by Telstra Wireless Access Services, Perth, Australia. Where possible, the transmitting power was verified by LOS measurements near the BS. The local average received power that was used in the analysis is computed by averaging signal measurements over a measurement track of 300 wavelengths, which corresponds to approximately 100 m. The typical traveling speed during the measurement was in the range of 80–100 km/h.

It is noted that the three BS stations A, B, and C are positioned within, or just outside, built-up areas (small business centers and large storage facilities). As can be seen in, e.g., Fig. 13, the received and measured pilot power is therefore typically affected by these obstacles for shorter antenna separation distances. Otherwise, the region where the measurement results were obtained can be classified as open farmland with occasional large trees branching overhead. It should also be noted that building and vegetation information were not included in the path loss predictions using the P.1546 models and that the measurement tracks are all within 28 km to the BS, i.e., within the size of a rural IS-95 cell.

### B. Statistical Analysis Metrics

First order statistics, correlation factor, and hit rate metrics have been used to evaluate the results.

*1) First Order Statistics:* The mean of the prediction error and its standard deviation are first order statistics that are traditionally used for evaluating the accuracy of prediction models. Here, predicted and measured values are denoted by  $p_i$  and  $m_i$ , respectively, and are given on a logarithmic (decibels) scale. The prediction error is expressed as

$$\epsilon_i = p_i - m_i, \quad i = 1, 2, \dots, N \quad (5)$$

where  $N$  is the number of samples corresponding to 300 wavelengths, as described in Section IV-A. The maximum prediction deviation from the measured values is calculated as

$$\epsilon_{max} = \max_{1 \leq i \leq N} \{|\epsilon_i|\} \quad (6)$$

and the mean prediction error is obtained as follows:

$$\bar{\epsilon} = \frac{1}{N} \sum_{i=1}^N \epsilon_i. \quad (7)$$

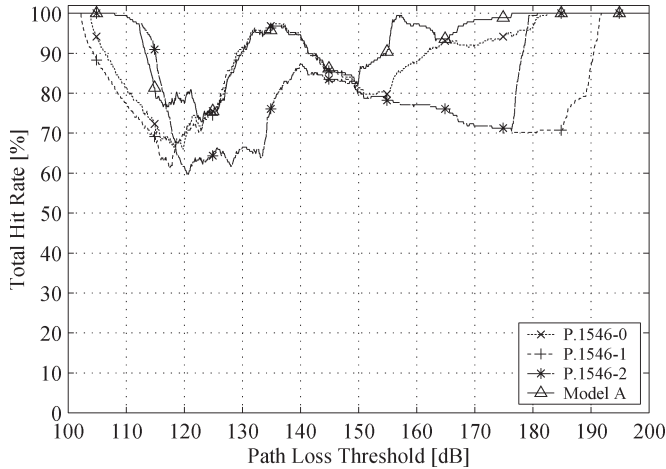


Fig. 9. Model comparison using THR and measurement 2003\_A1. The AHRE results for P.1546-0, P.1546-1, P.1546-2, and Model A are 13.43%, 20.64%, 22.26%, and 9.52%, respectively.

Finally, the prediction error's standard deviation is calculated as

$$\sigma_\epsilon = \sqrt{\frac{\sum_{i=1}^N (\epsilon_i - \bar{\epsilon})^2}{N-1}}. \quad (8)$$

2) *Correlation Coefficient*: The correlation coefficient provides a measure of the degree of linear relationship between two random variables and is calculated as

$$r_\epsilon = \frac{\sum_{i=1}^N (m_i - \bar{m})(p_i - \bar{p})}{\sqrt{\sum_{i=1}^N (m_i - \bar{m})^2} \sqrt{\sum_{i=1}^N (p_i - \bar{p})^2}} \quad (9)$$

where  $\bar{m}$  and  $\bar{p}$  are the means of the measured and predicted values, respectively. A correlation coefficient that is close to 1 indicates a strong linear relationship.

3) *Total Hit Rate*: When determining the accuracy of a prediction model, hit rate metrics [21] may be used to complement the first order statistics and the correlation factor. In this paper, the location-specific total hit rate (THR) is used as a direct indication of the quality of the prediction model. Given a path loss threshold  $L_T$ , if both the predicted and measured path loss values are greater than, less than, or equal to  $L_T$ , the prediction is regarded as correct, irrespective of the deviation of the predicted from the measured value. The method is useful in assessing the validity of a model where coverage is determined simply by a threshold value. For further details on the hit rate metrics, see [21]. To compare the different models using THR, the average total hit rate error (AHRE) was introduced in [19]. AHRE is the mean deviation from 100% THR and is expressed as

$$\text{AHRE} = \frac{1}{N_{L_T}} \sum_{L_T=L_{T,\min}}^{L_{T,\max}} 100\% - \text{THR}(L_T) \quad (10)$$

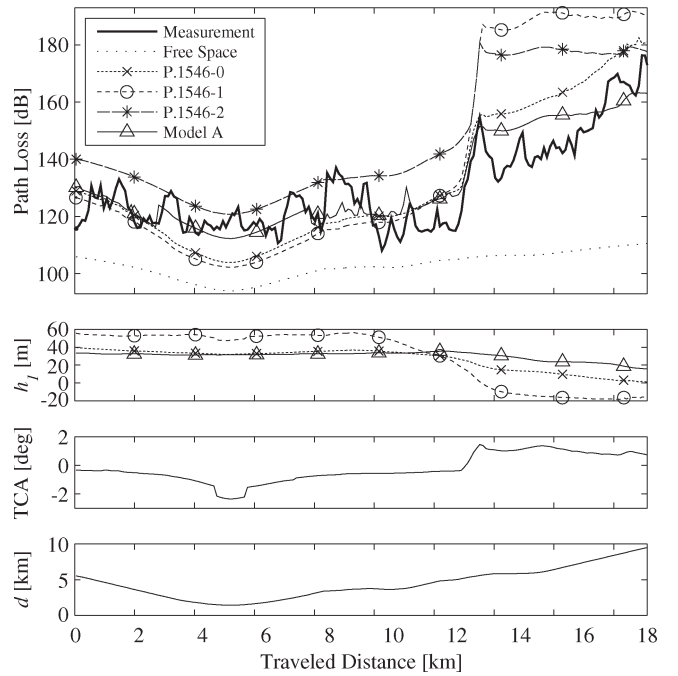


Fig. 10. Measurement 2003\_A1 around Beverley BS, where the transmitting/base antenna height is negative for some parts of the route.

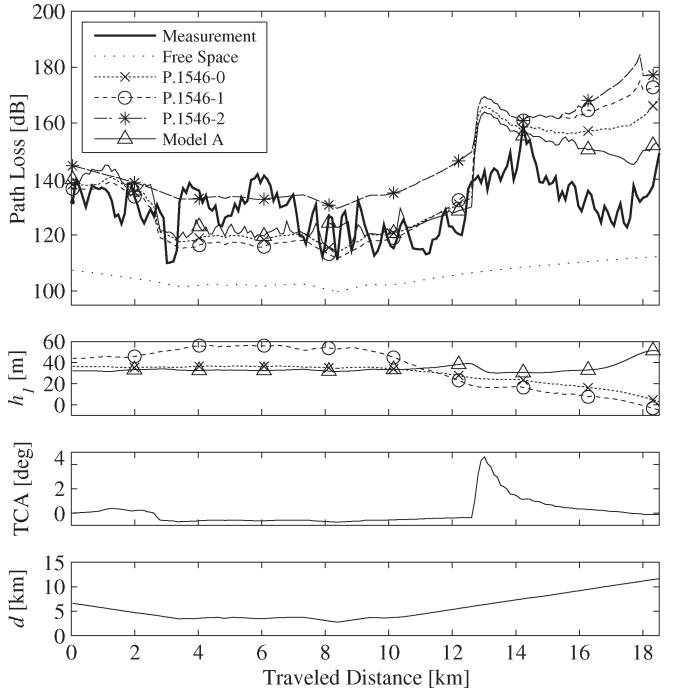


Fig. 11. Measurement 2004\_A5 around Beverley BS with negative transmitting/base antenna height and TCA correction overshoot at a traveled distance of approximately 13 km.

where  $L_T$  is the path loss threshold, and  $N_{L_T}$  is the number of THR points. A small value of AHRE indicates a good fit between the predicted and estimated values. In this paper,  $L_{T,\min}$  and  $L_{T,\max}$  are chosen, so that AHRE may be interpreted as the area between the THR curve and 100% (see Fig. 9). Furthermore, path loss threshold  $L_T$  is increased from  $L_{T,\min}$  to  $L_{T,\max}$  in 0.1 dB steps.

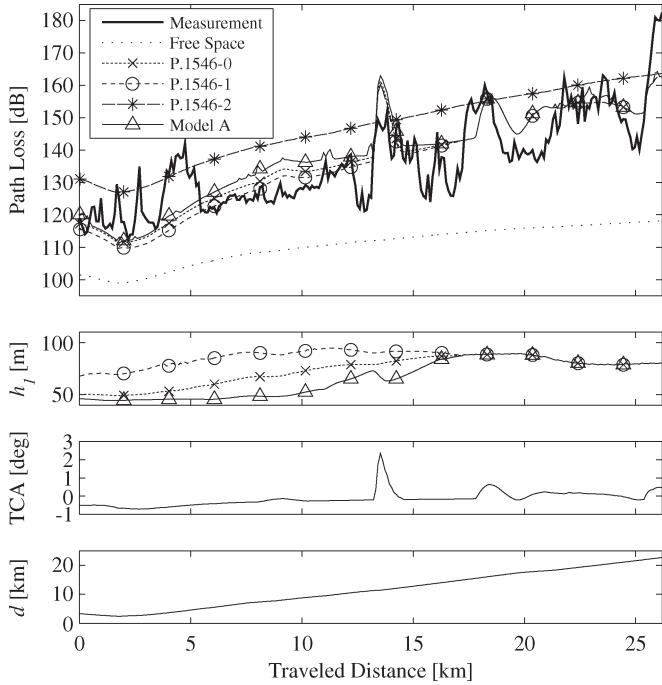


Fig. 12. Measurement 2004\_B8 around Quairading BS with TCA correction overshoot at a traveled distance of approximately 13 km.

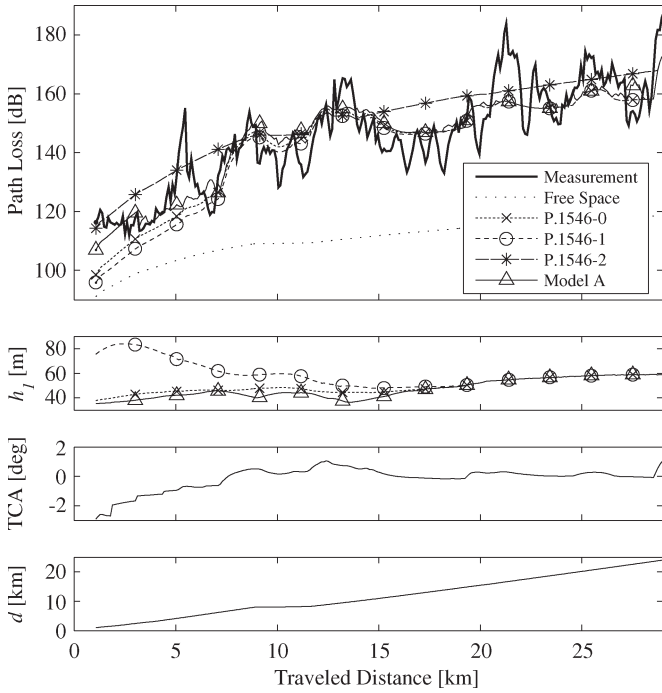


Fig. 13. Measurement 2003\_C1 around Corrigin BS spanning over 1–24 km to the BS.

### C. Results

Here, the P.1546 models are evaluated using the measurement data that were described in Section IV-A. Figs. 10–13 show four examples of path loss prediction versus traveled distance for the P.1546 versions. The figures also show Model A, which incorporates the authors' proposed modifications and is introduced later in Section V. The free space model is given as a path loss boundary, and  $h_1$  and TCA are shown in the

figures to reveal how the different algorithms produce different parameter values. In particular, it can be seen how the difference in the application of TCA correction (P.1546-1 and P.1546-2) affects the final prediction results, with P.1546-2 providing overall higher path loss predictions. Furthermore, the different  $h_1$  definitions (P.1546-0 and P.1546-1) reflect a small difference in the path loss predictions, which in, e.g., Fig. 13, is noticeable (2–3 dB) up to a traveled distance of about 8 km.

The statistical analysis summary for the P.1546 models is shown in Tables I and II. The statistical analysis metrics  $\epsilon_{max}$ ,  $\bar{\epsilon}$ ,  $\sigma_\epsilon$ ,  $r_\epsilon$ , and AHRE for the P.1546 models and all measurements ranging from 2003\_A1 to 2004\_C5 are presented in Tables I and II. This notation describes when and where the measurements were obtained [year (2003/2004), BS (A/B/C), and route index]. Furthermore, the last row in each table presents the average prediction results for all measurements that were calculated per model and statistical analysis metric. The results show that the P.1546-0 model provides the overall best predictions ( $\epsilon_{max}$ ,  $\bar{\epsilon}$ ,  $r_\epsilon$ , and AHRE) of the three P.1546 versions.

As shown in Table I, the average of the maximum prediction deviation over all 19 measurements (from 2003\_A1 to 2004\_C5) is of similar order for all three P.1546 models, namely, 25.52, 28.87, and 29.77 dB for P.1546-0, P.1546-1, and P.1546-2, respectively. On the other hand, the average of the mean prediction errors for the P.1546-0 and the P.1546-1 models are  $-0.26$  and  $-1.23$  dB, respectively, which can be considered to be very good compared with the average of the mean prediction error of 11.11 dB for the P.1546-2 model. As such, the P.1546-2 model, on average, predicts 11.37 dB and 12.34 dB higher path loss than P.1546-0 and P.1546-1, respectively, mainly due to the fact that TCA correction is not applied in P.1546-2 for  $\theta_{tca} < 0.55^\circ$ . In other words, the path loss predictions of P.1546-0 and P.1546-1 follow the trends in the measurements better than that of the P.1546-2 model, because of how the TCA correction is applied (see Section II-C). However, P.1546-2 provides the lowest average standard deviation of 8.71 dB of the P.1546 versions. Again, this is thought to be the case, because TCA correction is applied only when the straight line between the transmitting and receiving antennas is obstructed.

As far as the prediction accuracy of the three P.1546 versions is concerned, it can be seen in Table II that P.1546-0 and P.1546-1 yield a slightly better average correlation coefficient ( $\bar{r}_\epsilon = 0.69$ ) than the P.1546-2 model ( $\bar{r}_\epsilon = 0.65$ ). This is the result of TCA correction being applied for both LOS and non-LOS scenarios. A more distinct differentiation among the three versions can be observed with respect to the total hit rate and average hit rate error. In particular, P.1546-0 provides the best overall AHRE results ( $\overline{\text{AHRE}} = 15.75\%$ ), where the small difference compared to P.1546-1 ( $\overline{\text{AHRE}} = 16.23\%$ ) originates from their different  $h_1$  definitions (see Section II-A). The P.1546-2 model produces the highest overall average hit rate error ( $\overline{\text{AHRE}} = 23.07\%$ ) and, hence, provides only inferior results compared to both P.1546-0 and P.1546-1. To illustrate this characteristic, Fig. 9 shows the THR curves for the representative example of measurement 2003\_A1, with the AHRE being the area between the THR curve and 100%.

TABLE I  
FIRST ORDER STATISTICS FOR THE P.1546-0, P.1546-1, AND P.1546-2 MODELS

Meas.	$\epsilon_{max}$ [dB]			$\bar{\epsilon}$ [dB]			$\sigma_{\epsilon}$ [dB]		
	P.1546-0	P.1546-1	P.1546-2	P.1546-0	P.1546-1	P.1546-2	P.1546-0	P.1546-1	P.1546-2
2003_A1	24.05	53.32	44.47	2.11	8.02	16.01	11.95	22.60	12.14
2003_A2	21.01	23.22	26.80	-3.76	-5.81	9.31	9.88	9.96	9.22
2004_A3	22.11	23.77	26.88	-0.83	-2.98	12.14	10.19	10.08	8.02
2004_A4	20.46	22.12	28.15	-0.60	-2.75	12.50	10.71	10.59	8.75
2004_A5	36.17	46.59	54.52	5.33	6.09	16.40	14.82	18.32	14.26
2003_B1	19.06	20.14	25.09	-4.62	-5.64	11.97	6.99	6.89	7.25
2003_B2	22.48	21.88	33.05	5.47	4.35	15.18	9.11	9.22	9.47
2003_B3	30.65	32.44	27.73	-2.73	-4.10	9.37	10.46	10.19	10.70
2004_B4	29.54	30.33	21.93	-7.88	-8.72	6.66	8.94	8.79	8.82
2004_B5	25.57	26.30	23.97	0.38	-0.43	9.65	6.77	7.07	6.35
2004_B6	17.26	16.78	27.38	6.59	6.02	14.02	5.35	5.46	5.59
2004_B7	23.43	24.09	20.56	-8.50	-9.90	5.74	8.02	7.68	6.21
2004_B8	22.56	24.51	27.70	1.41	0.30	11.04	8.34	8.60	8.29
2004_B9	25.19	25.22	31.26	-0.81	-2.08	11.05	10.35	10.34	8.85
2003_C1	34.37	37.09	25.00	-2.19	-3.29	4.94	8.54	8.85	8.90
2004_C2	26.57	29.33	30.41	2.24	0.27	11.26	9.53	9.97	8.33
2004_C3	29.58	31.62	28.49	1.55	-0.71	12.31	9.00	8.98	7.98
2004_C4	30.22	32.26	34.44	2.87	0.54	14.72	10.13	10.25	7.73
2004_C5	24.68	27.59	27.73	-1.01	-2.63	6.79	9.27	9.91	8.58
Average	25.52	28.87	29.77	-0.26	-1.23	11.11	9.39	10.20	8.71

TABLE II  
CORRELATION COEFFICIENT AND AHRE FOR  
THE P.1546-0, P.1546-1, AND P.1546-2 MODELS

Meas.	$r_{\epsilon}$			AHRE [%]		
	P.1546-0	P.1546-1	P.1546-2	P.1546-0	P.1546-1	P.1546-2
2003_A1	0.89	0.85	0.84	13.43	20.64	22.26
2003_A2	0.61	0.60	0.53	15.26	15.98	19.57
2004_A3	0.37	0.38	0.28	25.34	24.01	35.15
2004_A4	0.27	0.28	0.15	25.85	24.72	36.66
2004_A5	0.56	0.52	0.45	21.64	23.16	23.16
2003_B1	0.64	0.65	0.59	19.01	20.03	29.05
2003_B2	0.83	0.83	0.81	10.91	10.14	19.76
2003_B3	0.74	0.76	0.72	11.22	11.06	16.51
2004_B4	0.68	0.69	0.63	16.70	17.62	18.13
2004_B5	0.76	0.76	0.73	12.43	12.74	21.64
2004_B6	0.69	0.69	0.62	22.74	21.84	41.23
2004_B7	0.59	0.59	0.60	23.04	25.09	20.12
2004_B8	0.83	0.83	0.81	9.59	9.15	17.36
2004_B9	0.70	0.71	0.65	14.90	15.22	22.84
2003_C1	0.88	0.88	0.86	7.88	8.17	11.29
2004_C2	0.78	0.78	0.76	12.79	12.44	21.11
2004_C3	0.74	0.75	0.72	11.28	10.65	21.25
2004_C4	0.64	0.65	0.68	15.65	15.58	28.20
2004_C5	0.86	0.86	0.81	9.52	10.18	13.14
Average	0.69	0.69	0.65	15.75	16.23	23.07

Apart from the aforementioned overall statistical characteristics, a number of other findings can be deduced from the individual measurements as follows: In particular, the P.1546-1 model severely overestimates ( $> 50$  dB) the path loss when  $h_1$  produces negative values for parts of some measurement routes (2003\_A1 and 2004\_A5), which can be seen in Figs. 10 and 11. This behavior also explains the large standard deviation  $\sigma_{\epsilon}$  of error for the associated predictions. In contrast, the P.1546-0 model handles the problem with negative  $h_1$  values better due to the fact that  $h_1$  is calculated, taking the physical height of the transmitting antenna into greater account (see Section II-A1). For the same scenarios, the P.1546-2 correction for negative  $h_1$  values slightly improves the prediction accuracy. This correction may result in a prediction discontinuity, which can be

seen in Fig. 11 at a traveled distance of approximately 18 km. It is also noted that path loss prediction overshoots originating from the TCA correction sometimes occur, which can clearly be seen in Figs. 11 and 12 at a traveled distance of approximately 13 km.

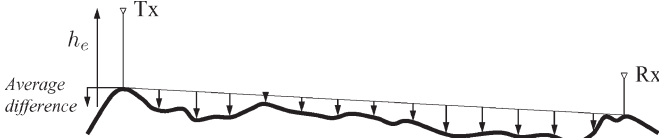
## V. DISCUSSIONS AND PROPOSED MODIFICATIONS

First, the results in Section IV-C show that the P.1546 models sometimes produce abnormal predictions due to the negative  $h_1$  values being produced (2003\_A1 and 2004\_A5). Therefore, a new transmitting/base antenna height definition  $h_1$  that remedies this behavior is proposed in Section V-A. Second, for the measurements that are presented in this paper, buildings and other man-made obstacles, resulting in increased path loss, are typically present for distances within about 2.5 km to the BS. In addition, vegetation along the measurement routes sometimes has a major impact on the received field strength. To increase the prediction accuracy, land usage and vegetation information should preferably be incorporated in the propagation model.

These modifications are therefore incorporated in our proposed Model A, which is described and evaluated in this section. The model is based on the P.1546 field strength curves;  $h_1$  is calculated, as shown in Section V-A, TCA correction is applied as in P.1546-1, and corrections for different land usage and vegetation surrounding the receiving antenna are introduced.

### A. Transmitting/Base Antenna Height Modification

The definition of effective antenna height, as in [4], which is used in P.1546 [11]–[13] to obtain the transmitting/base antenna height, is widely used and accepted, albeit it has known limitations. For example, for shorter transmitting and receiving antenna separation distances where both antennas are positioned on the same slope, this definition might produce negative  $h_1$

Fig. 14. Alternative definition of effective antenna height  $h_e$ .

values. Even though this is a well-known shortcoming, a simple solution has yet to be presented and accepted. In addition, it is noted that the standard definition is not reciprocal, which is one of the basic requirements from the mobile community point of view. For a mobile telephony scenario, this means that the BS-to-mobile (downlink) predictions should preferably be equal to the mobile-to-BS (uplink) predictions. In this section, the proposed  $h_1$  definition that deals with the negative transmitting/base antenna height problem is presented. Scenarios where negative  $h_1$  values sometimes may occur are also presented and discussed.

1) *Alternative Effective Antenna Height Definition  $h_e$* : The effective height of the base antenna,  $h_e$  is defined as the average difference of terrain height relative to a line connecting the ground levels at transmitting and receiving antennas subtracted from the height of the transmitting antenna  $h_{tx}$ , (see Fig. 14 and [22] and [23]). In practice, this definition mitigates the problems with both negative values and reciprocity.

2) *Scenarios*: The  $h_{eff}$  definition, as in the P.1546 models, sometimes results in negative  $h_1$  values when the receiving antenna is located on a slope and the transmitting/base antenna is located below [see Fig. 15(a)]. This, in turn, sometimes results in an unrealistic underestimation of the field strength, as previously shown in Section IV-C and Figs. 10 and 11. If the transmitting and receiving antennas change positions,  $h_e$  remains the same, as shown in Fig. 15(a) and (b). On the other hand, for longer distances where the transmitting antenna is located on an isolated height, as in a typical broadcasting situation, the traditional method appears to be more realistic (at least in one direction) (see Fig. 16). The explanation for this is that, if the path is relatively flat from transmitter to receiver and the transmitting antenna is mounted on a high mast, the propagation characteristics may be very similar to the transmitter being on a lower mast that is located on a hill.

3) *Proposed Definition*: To obtain an  $h_1$  definition that can be accepted by both broadcasting and mobile communications users, we propose that the effective antenna height definition  $h_{eff}$  be used for distances that are greater than 15 km. For antenna separations  $d$  that are less than 15 km, the alternative effective antenna height definition  $h_e$ , which was given in Section V-A1, should preferably be used. To avoid a discontinuity at the transition at 15 km, the resulting effective antenna height should be interpolated from  $h_e$  and  $h_{eff}$ . Therefore, a transition effective antenna height may be calculated as

$$h_t = \frac{(h_b - h_e)d + 15h_e - 12h_b}{3} \quad (11)$$

for distances within the range of 12–15 km. In (11), antenna heights  $h_b$ ,  $h_e$ , and  $h_t$ , and distance  $d$  are given in meters and kilometers, respectively.

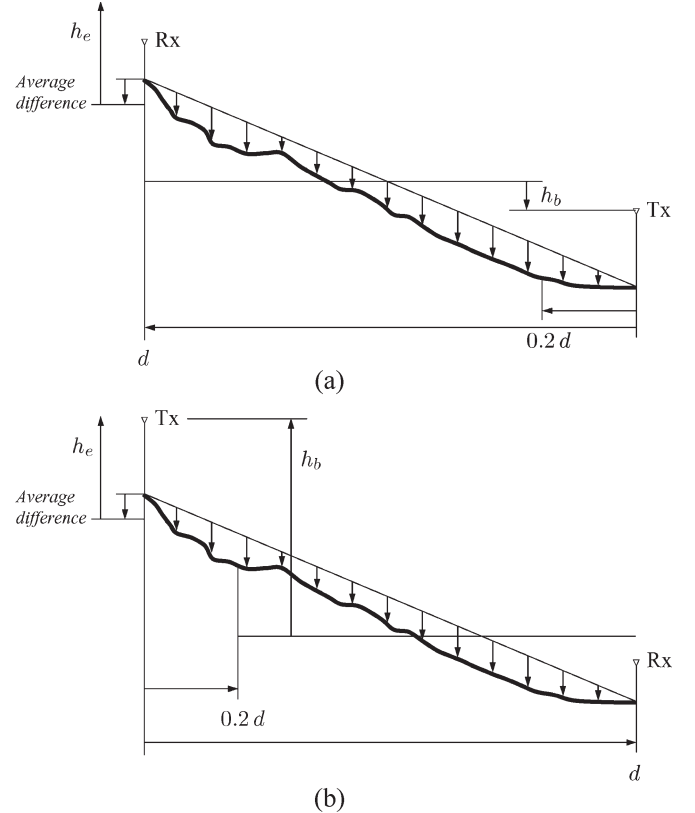
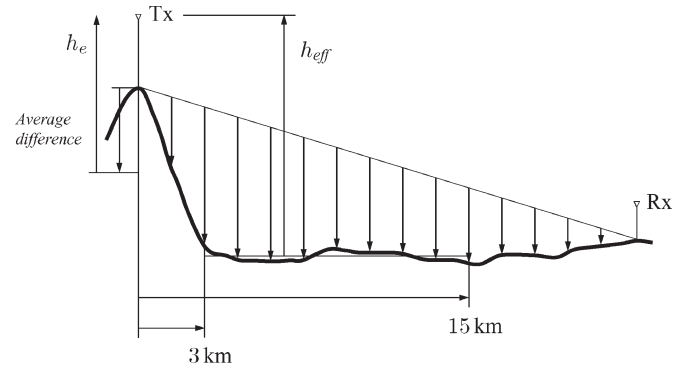
Fig. 15. Short-range ( $d < 15$  km) same-slope scenario. (a) Transmitting antenna positioned below the receiving antenna, resulting in negative transmitting/base antenna height. (b) Reverse scenario.

Fig. 16. Typical broadcasting situation with the transmitting antenna located on an isolated height.

In this paper, the 12 km limit has been chosen based on the available measurement data and may be updated when more data originating from diverse terrains become available for comparison.

It is known that the approach that was used in P.1546-0 to calculate  $h_1$  is more robust (i.e., less prone to produce negative  $h_1$  values) than the method that was used in P.1546-1 and P.1546-2. Therefore,  $h_1$  is calculated as

$$h_1 = \begin{cases} h_{tx} + \frac{(h_e - h_{tx})d}{15}, & \text{for } 1 \text{ km} \leq d < 12 \text{ km}, \\ h_{tx} + \frac{(h_t - h_{tx})d}{15}, & \text{for } 12 \text{ km} \leq d < 15 \text{ km}, \\ h_{eff}, & \text{for } 15 \text{ km} \leq d \leq 1000 \text{ km}. \end{cases} \quad (12)$$

TABLE III  
VEGETATION TYPES

VT	Description
2	Shrublands; scrub-heath
3	Medium woodland; York gum, wandoo and salmon gum
6	Shrublands; scrub-heath
7	Medium woodland; York gum
8	Medium woodland; wandoo
18	Succulent steppe, sparse woodland and thicket; York gum
19	Shrublands; thicket with scattered wandoo
23	Medium woodland; wandoo, York gum and salmon gum
24	Shrublands; scrub-heath
29	Medium woodland; York gum and salmon gum

This definition (12) was proposed in [24] and is used in this paper for Model A path loss predictions.

### B. Land Usage and Vegetation Information

To further enhance Model A, land usage and vegetation information are incorporated in the predictions. Land usage has been implemented using the correction for the RAH (see Section II-B), which is already available in the P.1546 models. In Section V-B4, a field strength attenuation factor as a function of the vegetation density in the vicinity of the receiving antenna is proposed by the authors. In Section IV, it was noted that the measured field strength is typically attenuated due to buildings near the BS. To gather information about land usage (built-up areas), satellite photos and notes that were made during the measurements were inspected. It was then concluded that in the measurements, the land usage could be considered as being built-up. This information was then used in the standard P.1546 correction for the RAH. The representative clutter height for the built-up areas was set to be 20 m.

Although the vegetation along the measurement routes is very sparse, it is clear that the vegetation surrounding the receiving antenna sometimes has a big impact on the received field strength. Therefore, an add-on field strength correction factor based on vegetation type and vegetation density is introduced and incorporated into Model A. In Section IV-C (e.g., Figs. 11 and 12 at a traveled distance of approximately 13 km), it can be seen that the TCA correction sometimes gives an overshoot in the path loss predictions for prominent terrain obstacles and shorter distances. It is therefore motivated to not apply further attenuation due to vegetation for  $\theta_{tca} > 0.55^\circ$ .

1) *Vegetation Type*: The vegetation type (VT) data that were used in the analysis were provided by the Department of Agriculture, Western Australia. The data are given on broadscale format and identifies vegetation types in patches that are larger than about 25 hectares. Furthermore, the data set contains information on two levels: 1) land-use data and 2) vegetation type (e.g., medium woodland and York gum). In the rural area where the measurements were performed, ten different vegetation types were identified, as shown in Table III. Attenuation factors are not available for all vegetation types, so for convenience, the

types were divided into two groups corresponding to woodland (3, 7, 8, 18, 23, and 29) and shrublands (2, 6, 19, and 24).

2) *Vegetation Density*: The vegetation density data that were used in the analysis were provided by the CSIRO Mathematical and Information Sciences and the Land Monitor Western Australia. The perennial crown density information is given on an accurate 25 m grid and is represented by a scalar value ranging from 0% to 100%, corresponding to no vegetation and dense vegetation, respectively. The crown density metric corresponds to the estimated percentage of land that is covered by the tree crown [25].

3) *Extracted Data*: The data that were extracted from the vegetation type database corresponds to the most occurring vegetation type within a 100 m by 100 m area (typically only one type). The vegetation density near the receiver (VDN) corresponds to the average vegetation density within a 100 m by 100 m area surrounding the receiving antenna.

4) *Vegetation Attenuation*: The attenuation of field strength due to vegetation is based on previous findings for tree attenuation at 869 MHz [26]. These experiments showed that single trees attenuated the received signal with 10–20 dB. The approach in this paper is to simply add a field strength attenuation factor (FSAF) in decibels, depending on vegetation type and vegetation density, as

$$\text{FSAF} = \begin{cases} \frac{\text{VDN} \cdot 20}{100}, & \text{for woodland} \\ \frac{\text{VDN} \cdot 10}{100}, & \text{for shrublands.} \end{cases} \quad (13)$$

It is noted that VDN rarely exceeds 50% for the areas under consideration, which means that the FSAF, most likely, will never overcorrect the predictions.

### C. Evaluation of Model A

The statistical analysis summary for Model A and the rural OH model is presented in Table IV. It can be seen from these results that Model A outperforms the rural OH model with respect to all considered statistics. Specifically, the OH path loss predictions are, on average, too optimistic by 8.65 dB, which is in agreement with, e.g., [18].

A comparison of the statistics of the three P.1546 versions in Tables I and II with the results for Model A in Table IV reveals that Model A produces more accurate predictions overall, compared to the P.1546 models. The averages for the maximum prediction error, the standard deviation, the correlation factor, and the total hit rate error with respect to the conducted 19 measurements are obtained as  $\bar{\epsilon}_{max} = 22.78$  dB,  $\bar{\sigma}_\epsilon = 8.19$  dB,  $\bar{r}_\epsilon = 0.71$ , and  $\overline{\text{AHRE}} = 14.76\%$ , respectively, and have clearly improved compared with those of the P.1546 models. The only statistic that does not improve compared with that of all three P.1546 versions is the average of the mean prediction error (1.95 dB). It should be noted that this result is still better than the average of the mean prediction error that was obtained by using the P.1546-2 model (11.11 dB) and is well within the measurement accuracy margin.

The advantage of the proposed definition of the transmitting/base antenna height  $h_1$ , as outlined in Section V-A, can be clearly seen in Figs. 10 and 11. While the P.1546

TABLE IV  
STATISTICS FOR MODEL A AND THE OH RURAL MODEL

Meas.	$\epsilon_{max}$ [dB]		$\bar{\epsilon}$ [dB]		$\sigma_\epsilon$ [dB]		$r_\epsilon$		AHRE [%]	
	Model A	OH	Model A	OH	Model A	OH	Model A	OH	Model A	OH
2003_A1	17.87	45.45	1.66	-12.42	7.73	11.37	0.89	0.75	9.52	18.35
2003_A2	18.23	34.18	-0.73	-8.53	8.50	9.54	0.67	0.49	13.83	16.52
2004_A3	17.36	23.95	3.38	-5.41	7.70	8.43	0.47	0.26	22.84	21.85
2004_A4	19.68	22.30	3.64	-5.08	8.14	9.18	0.39	0.13	23.78	23.00
2004_A5	27.26	31.62	4.73	-8.31	11.46	8.81	0.61	0.45	19.39	20.09
2003_B1	15.28	22.90	-2.19	-7.94	5.83	7.34	0.77	0.59	13.94	24.04
2003_B2	23.50	42.74	6.84	-4.07	9.31	10.34	0.82	0.78	12.10	9.55
2003_B3	31.18	49.16	-0.52	-10.08	10.24	11.95	0.75	0.62	10.68	14.40
2004_B4	29.23	36.98	-4.70	-13.63	6.80	9.21	0.80	0.59	11.95	24.50
2004_B5	25.28	33.28	1.85	-10.16	6.84	6.44	0.74	0.71	13.17	24.22
2004_B6	18.95	18.42	8.39	-5.45	5.82	5.90	0.59	0.58	26.91	22.36
2004_B7	18.68	26.39	-4.63	-13.63	6.90	6.72	0.58	0.59	19.59	30.17
2004_B8	21.99	41.36	2.76	-8.22	8.44	9.04	0.82	0.77	10.55	12.22
2004_B9	22.08	32.96	1.33	-8.12	9.54	9.72	0.71	0.58	14.08	16.53
2003_C1	31.08	45.43	-0.26	-15.75	8.33	9.76	0.87	0.84	8.18	17.43
2004_C2	24.53	30.36	4.93	-7.24	8.41	8.52	0.81	0.75	13.62	13.53
2004_C3	21.11	32.01	4.35	-4.89	8.03	8.58	0.76	0.68	12.37	11.23
2004_C4	27.56	32.65	4.71	-2.63	9.35	8.20	0.67	0.65	14.64	13.50
2004_C5	22.01	40.60	1.48	-12.76	8.15	8.74	0.86	0.80	9.24	15.94
Average	22.78	33.83	1.95	-8.65	8.19	8.83	0.71	0.61	14.76	18.39

models tend to significantly overestimate the path loss for those parts of the measurement routes where negative or small  $h_1$  values occur, this problem is less severe with Model A. For instance, it can be seen in Fig. 10, at a traveled distance of approximately 13 km, that the proposed definition of  $h_1$ , as described in Section V-A3, quite drastically remedies the prediction overshoot problem with negative  $h_1$  values. The statistical results support the conclusion that there are no obvious shortcomings for normal scenarios using the definition of the transmitting/base antenna height  $h_1$ , as proposed in (12).

Another factor behind the improvement in the overall prediction results for Model A, as shown in Table IV, is given by the incorporation of land usage and the vegetation attenuation factor. The addition of land usage (buildings) for shorter distances makes the predictions more accurate (see, e.g., Fig. 10 for traveled distances between 2.8 and 7.9 km). In addition, the prediction results improve when using the vegetation correction, which can be seen in, e.g., Fig. 11 at a traveled distance in the range of 4–7 km.

## VI. CONCLUSION

In this paper, the validity of the three versions of Recommendation ITU-R P.1546 for path loss prediction in rural Australia has been analyzed. Specifically, versions P.1546-0, P.1546-1, and P.1546-2 are compared against simple models and evaluated using measurement results that were obtained by utilizing the pilot signal of a commercial CDMA mobile telephone network. It is shown that P.1546-0 and P.1546-1 provide better overall prediction of path loss compared to traditional models, such as the Okumura–Hata model. The comparison with the measurement results also shows that P.1546-2, on average, underestimates the field strength by more than 10 dB for typical Australian rural areas. However, it is found that P.1546-2 improves the standard deviation of the prediction error

compared to previous versions of the Recommendation. As the P.1546 models cater for corrections for both RAH and TCA, additional accuracy to the predictions can generally be achieved.

The evaluation of the three P.1546 versions has revealed some degradation in prediction performance in cases when negative values of transmitting/base antenna height  $h_1$  are produced. Specifically, it is noted that the method that was used in P.1546-0 to calculate  $h_1$  is more accurate and robust toward the processing of negative  $h_1$  values than the method that was used in the successor versions P.1546-1 and P.1546-2. This shortcoming is typically observed as a severe overestimation of the path loss in some scenarios (see Figs. 10 and 11). To remedy this problem, a modification of the transmitting/base antenna height  $h_1$  definition is proposed in this paper. This  $h_1$  definition incorporates the effective height  $h_e$  of the BS for distances  $d < 15$  km and uses the well-established effective antenna height  $h_{eff}$  for distances  $d \geq 15$  km [see (12)]. It is shown that a considerable improvement in prediction accuracy can be achieved in scenarios where, otherwise, a path loss overestimation due to negative  $h_1$  values will occur (see Figs. 10 and 11).

Additional improvements can be obtained by incorporating land usage and vegetation information into the path loss predictions to cater to field strength attenuation due to buildings and vegetation at the receiving antenna. These factors, together with the aforementioned proposed definition of the transmitting/base antenna height, are consolidated into Model A. In summary, Model A provides more accurate and reliable path loss predictions for the rural areas that were tested than the P.1546 models and the rural OH model. Additional comparisons with measurement data to be obtained in different rural areas are needed to further prove Model A's universal applicability.

Although a significant amount of work has been performed and incorporated into the development of Recommendation ITU-R P.1546 since its incarnation in 2001, such as

methods for mixed land/sea paths and short urban/suburban paths, additional efforts are still needed to obtain a model that can be widely applied for a large variety of scenarios. For example, this paper shows that the latest version P.1546-2 severely underestimates the field strength when tested against measurement results for short range (typically less than 20 km) and rural scenarios. The implication is that both TCA correction and RAH correction in these scenarios can be very much dependent on the distance to the BS. To develop reliable distance-dependent correction models, a large quantity of measurement data originating from different types of terrain should be obtained and analyzed in future work.

#### ACKNOWLEDGMENT

The authors would like to thank U. Engelke and A. Pollok for their assistance with the measurement campaigns; Telstra Wireless Access Services for providing the BS characteristics; J. Wallace and Dr. J. Chia of CSIRO Mathematical and Information Sciences and Land Monitor, Western Australia, respectively, for providing the digital vegetation density data; D. Shepherd of the Department of Agriculture, Western Australia, for making the vegetation type database available; and the anonymous reviewers for their valuable comments.

#### REFERENCES

- [1] K. Bullington, "Radio propagation at frequencies above 30 mega-cycles," *IRE*, vol. 35, no. 10, pp. 1122–1136, Oct. 1947.
- [2] K. Bullington, "Radio propagation for vehicular communications," *IEEE Trans. Veh. Technol.*, vol. VT-26, no. 4, pp. 295–308, Nov. 1977.
- [3] A. G. Longley and P. L. Rice, "Prediction of tropospheric radio transmission over irregular terrain-A computer method-1968," U.S. Gov. Printing Office, Washington, DC, ESSA Tech. Rep. ERL 79-ITS 67, Jul. 1968.
- [4] Y. Okumura, E. Ohmohri, T. Kawano, and K. Fukada, "Field strength and its variability in VHF and UHF land-mobile radio service," *Rev. Electr. Commun. Labs.*, vol. 16, no. 9–10, pp. 825–873, Sep. 1968.
- [5] H. Bertoni, Ed., "Coverage prediction for mobile radio systems operating in the 800/900 MHz frequency range," *IEEE Trans. Veh. Technol.*, vol. 37, no. 1, pp. 3–72, Feb. 1988.
- [6] R. J. Luebers, "Propagation prediction for hilly terrain using GTD wedge diffraction," *IEEE Trans. Antennas Propagat.*, vol. AP-32, no. 9, pp. 951–955, Sep. 1984.
- [7] G. A. Hufford, "An integral equation approach to the problem of wave propagation over an irregular surface," *Quart. J. Mech. Appl. Math.*, vol. 9, no. 4, pp. 391–404, Jan. 1952.
- [8] C. A. Zelley and C. C. Constantinou, "A three-dimensional parabolic equation applied to VHF/UHF propagation over irregular terrain," *IEEE Trans. Antennas Propagat.*, vol. 47, no. 10, pp. 1586–1596, Oct. 1999.
- [9] *VHF and UHF Propagation Curves for the Frequency Range From 30 MHz to 1000 MHz*, Oct. 1999. ITU-R Recommendation P.370-7.
- [10] *Prediction Methods for the Terrestrial Land Mobile Service in the VHF and UHF Bands*, Oct. 1995. ITU-R Recommendation P.529-3.
- [11] *Method for Point-to-Area Predictions for Terrestrial Services in the Frequency Range 30 MHz to 3000 MHz*, Oct. 2001. ITU-R Recommendation P.1546.
- [12] *Method for Point-to-Area Predictions for Terrestrial Services in the Frequency Range 30 MHz to 3000 MHz*, Apr. 2003. ITU-R Recommendation P.1546-1.
- [13] *Method for Point-to-Area Predictions for Terrestrial Services in the Frequency Range 30 MHz to 3000 MHz*, Sep. 2005. ITU-R Recommendation P.1546-2.
- [14] T. S. Rappaport, *Wireless Communications: Principles and Practice*. New York: Prentice-Hall, 1996.
- [15] "Mobile station-base station compatibility standard for dual-mode wideband spread spectrum cellular system," in *Proc. Telecommun. Industry Assoc.*, Washington, DC, Jul. 1993. TIA/EIA/IS-95.
- [16] M. Hata, "Empirical formula for propagation loss in land mobile radio services," *IEEE Trans. Veh. Technol.*, vol. VT-29, no. 3, pp. 317–325, Aug. 1980.
- [17] *The Prediction of Field Strength for Land Mobile and Terrestrial Broadcasting Services in the Frequency Range From 1 to 3 GHz*, Oct. 1999. ITU-R Recommendation P.1146.
- [18] J. D. Parsons, *The Mobile Radio Propagation Channel*. Chichester, U.K.: Wiley, 2000.
- [19] E. Östlin, H.-J. Zepernick, and H. Suzuki, "Evaluation of the new semi-terrain based propagation model Recommendation ITU-R P.1546," in *Proc. IEEE Semiannual Veh. Technol. Conf.*, Orlando, FL, Oct. 2003, vol. 1, pp. 114–118.
- [20] E. Östlin, H.-J. Zepernick, and H. Suzuki, "Macrocell radio wave propagation prediction using an artificial neural network," in *Proc. IEEE Semiannual Veh. Technol. Conf.*, Los Angeles, CA, 2004, vol. 1, pp. 57–61.
- [21] A. S. Owadally, E. Montiel, and S. R. Saunders, "A comparison of the accuracy of propagation models using hit rate analysis," in *Proc. IEEE Semiannual Veh. Technol. Conf.*, Atlantic City, NJ, 2001, vol. 4, pp. 1979–1983.
- [22] *Effect on Prediction Accuracy Using New Definition of Effective Transmitting/Base Antenna Height in Recommendation ITU-R P.1546-1*, Sep. 2004. ITU-R Input Document 3K/39-E.
- [23] *Proposed Modification to Recommendation ITU-R P.1546-2*, Sep. 2005. ITU-R Input Document 3K/72-E.
- [24] E. Östlin, H. Suzuki, and H.-J. Zepernick, "Evaluation of a new effective antenna height definition in ITU-R Recommendation P.1546," in *Proc. 11th Asia-Pacific Conf. Commun.*, Perth, Australia, Oct. 2005, pp. 128–132.
- [25] S.-M. Lee, N. A. Clark, and P. A. Araman, "Automated methods of tree boundary extraction and foliage transparency estimation from digital imagery," in *Proc. 19th Biennial Workshop Color Photography Videography Airborne Imaging Resource Assessment*, Logan, UT, 2004.
- [26] W. J. Vogel and J. Goldhirsh, "Tree attenuation at 869 MHz derived from remotely piloted aircraft measurements," *IEEE Trans. Antennas Propagat.*, vol. AP-34, no. 12, pp. 1460–1464, Dec. 1986.



**Erik Östlin** (S'06) received the B.S. degree in electrical engineering from Högskolan Dalarna, Falun, Sweden, in 1999 and the M.S. degree in electrical engineering, with emphasis on signal processing and telecommunications, in 2001, from Blekinge Institute of Technology, Ronneby, Sweden, where he is currently working toward the Licentiate degree. He finished his M.S. project at the Australian Telecommunications Research Institute, Bentley, Australia.

Shortly after, he was invited to join the Australian Telecommunications Cooperative Research Centre Wideband CDMA Scanner Project, Perth, Australia. Since April 2006, he has been a Digital Signal Processing Engineer with Sensear Pty. Ltd., Perth.



**Hajime Suzuki** (S'94–M'99) received the B.E. and M.E. degrees from the University of Electro-Communications, Tokyo, Japan, in 1993 and 1995, respectively, and the Ph.D. degree from the University of Technology, Sydney, Australia, in 1999.

In 1999, he joined the Division of Telecommunications and Industrial Physics, Commonwealth Scientific and Industrial Research Organisation (CSIRO), Marsfield, Australia, and was transferred to the CSIRO Information and Communication Technologies Centre in 2003. He is an active participant of the Australian Radio Communication Study Group 3 and of the Study Group 3 (Radio Propagation), International Telecommunication Union Radiocommunication Sector (ITU-R), particularly, of the Working Party 3K (point-to-area propagation). He is also the Chairman of the Subgroup 3K-3 on indoor and short-range propagation.

Authorized licensed use limited to: CSIRO LIBRARY SERVICES. Downloaded on August 26, 2009 at 19:02 from IEEE Xplore. Restrictions apply.



**Hans-Jürgen Zepernick** (M'94) received the Dipl.-Ing. degree in electrical engineering from the University of Siegen, Siegen, Germany, in 1987 and the Dr.-Ing. degree from the University of Hagen, Hagen, Germany, in 1994.

He is currently a Professor and the Chair of radio communications at the School of Engineering, Blekinge Institute of Technology (BTH), Ronneby, Sweden. Prior to his appointment at BTH in October 2004, he held the positions of Professor of wireless communications at Curtin University of Technology, Perth, Australia; Deputy Director of the Australian Telecommunications Research Institute (ATRI); and Associate Director of the Australian Telecommunications Cooperative Research Centre (ATcrc). He was the Leader of ATcrc's wireless program and the Leader of the center's radio transmission technology project. He served on the Board of Management of ATRI and the Executive Research Committee of the ATcrc. He has been an active participant with the Wireless World Research Forum and is actively involved in the European FP6 Network of Excellence *EuroFGI*. He is the author or coauthor of some 110 technical papers and five book chapters in the areas of wireless and radio communications. He is also the lead author of the textbook entitled *Pseudo Random Signal Processing: Theory and Application* (Wiley, 2005). His research interests include radio channel characterization and modeling, coding and modulation, equalization, spread-spectrum systems, mobile multimedia communications, and future-generation wireless systems.